Phase diagrams and crossover in spatially anisotropic $d=3$ Ising, XY magnetic, and percolation systems: Exact renormalization-group solutions of hierarchical models

Aykut Erbaş,[1] Aslı Tuncer,[1] Burcu Yücesoy,[1] and A. Nihat Berker[1,2,3]
[1]*Department of Physics, Istanbul Technical University, Maslak 34469, Istanbul, Turkey*
[2]*Department of Physics, Massachusetts Institute of Technology, Cambridge, Massachusetts 02139, USA*
[3]*Feza Gürsey Research Institute, TÜBITAK—Bosphorus University, Çengelköy 81220, Istanbul, Turkey*
(Received 17 May 2005; published 24 August 2005)

Hierarchical lattices that constitute spatially anisotropic systems are introduced. These lattices provide exact solutions for hierarchical models and, simultaneously, approximate solutions for uniaxially or fully anisotropic $d=3$ physical models. The global phase diagrams, with $d=2$ and $d=1$ to $d=3$ crossovers, are obtained for Ising and XY magnetic models and percolation systems, including crossovers from algebraic order to true long-range order.

DOI: 10.1103/PhysRevE.72.026129 PACS number(s): 64.60.Ak, 05.45.Df, 75.10.Hk, 05.10.Cc

I. INTRODUCTION

Spatially anisotropic systems greatly enrich our experience of collective phenomena, as exemplified by high-T_c superconducting materials, in which the couplings along one direction are much weaker than those in the perpendicular plane. Anisotropic systems are also intriguing from a conceptual point of view, since vastly different critical phenomena are known to happen in different spatial dimensions, whereas, between d-dimensional systems stacked along a new direction, even the weakest coupling, while not affecting the critical temperature, induces $(d+1)$-dimensional critical behavior. Calculational results that yield the global phase diagram of anisotropic systems and thus provide a unified connected picture of the various anisotropic and isotropic behaviors at different subdimensions and at the full dimension have been rare and mostly confined to $d=2$. In the present study, we obtain global phase diagrams for a variety of anisotropic $d=3$ systems: Ising magnetic, XY magnetic, and percolation systems. Anisotropy along one direction (uniaxial) and full anisotropy, in which the couplings along each direction are different, are studied, yielding global phase diagrams. We use hierarchical models, which yield exact renormalization-group solutions [1–3]. Thus, the construction of hierarchical lattices that incorporate correct dimensional reductions is an important step of the study. The exact solutions of hierarchical models can simultaneously be considered approximate position-space renormalization-group solutions of models on naturally occurring lattices [1]. The method developed in this study will be employed to extend, from isotropic to anisotropic systems, the renormalization-group solutions of the tJ and Hubbard models of electronic conduction [4–6].

II. ANISOTROPIC HIERARCHICAL LATTICES

Hierarchical lattices are constructed by repeatedly self-embedding a graph. These provide exactly solvable models, with which complex problems can be studied and understood. For example, frustrated [7], spin-glass [8], random-bond [9] and random-field [10], Schrödinger equation [11], lattice-vibration [12], dynamic scaling [13], aperiodic magnet [14], complex phase diagram [15], and directed-path [16] systems, etc., have been solved on hierarchical lattices.

In this study, we construct anisotropic hierarchical lattices by the parallel, mutual embeding of several graphs. In each embedding step, b and b^d, respectively, are the length and volume rescaling factors. We illustrate the method by the simplest case of the anisotropic $d=2$ lattice, before moving on to the uniaxially or fully anisotropic $d=3$ lattices. The parallel, mutual embeddings of the two graphs shown in Fig. 1 provide an anisotropic $d=2$ hierarchical lattice. If either of the couplings (K_x,K_y) is set to zero, the remaining coupling constitutes a one-dimensional lattice. When the couplings are of equal strength, $K_x=K_y$, the two directions, represented by the two embedding sequences, are equivalent and the lattice is isotropic $d=2$. This lattice will be referred to as A_2.

It is thus seen that generally our requirements in the construction of anisotropic hierarchical lattices are (1) the proper reduction to the lower dimension when one (or more, see

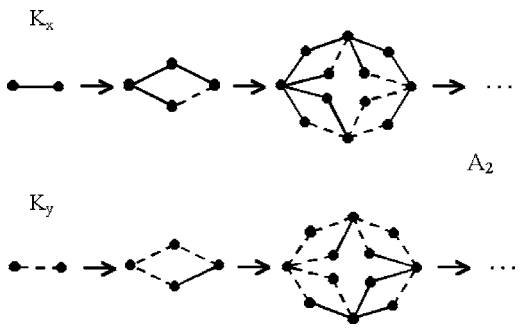

FIG. 1. The parallel, mutual embeddings of these two graphs provide an anisotropic $d=2$ hierarchical lattice. If either of the couplings (K_x,K_y) is set to zero, the remaining coupling constitutes a one-dimensional lattice. When the couplings are of equal strength, $K_x=K_y$, the two directions, represented by the two embedding sequences, are equivalent and the lattice is isotropic $d=2$. This lattice will be referred to as A_2.

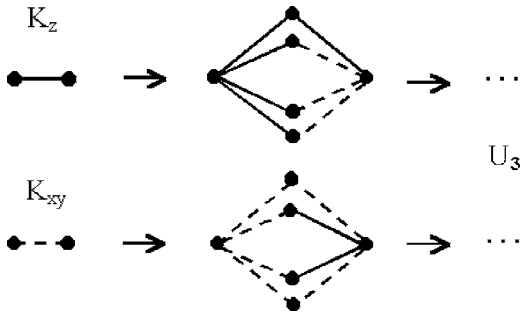

FIG. 2. The parallel, mutual embeddings of these two graphs provide a uniaxially anisotropic $d=3$ hierarchical lattice. If the coupling K_z is set to zero, the coupling K_{xy} constitutes an isotropic two-dimensional lattice. If the coupling K_{xy} is set to zero, the coupling K_z constitutes a one-dimensional lattice. When the couplings are of equal strength, $K_{xy}=K_z$, the z direction, represented by the first embedding sequence, and the x,y directions, represented by the second embedding sequence, are all equivalent and the lattice is isotropic $d=3$. This lattice will be referred to as U_3.

below) of the couplings is set to zero and (2) the restitution of an isotropic lattice when the couplings are of equal strength.

The parallel, mutual embeddings of the two graphs shown in Fig. 2 provide a uniaxially anisotropic $d=3$ hierarchical lattice. If the coupling K_z is set to zero, the coupling K_{xy} constitutes an isotropic two-dimensional lattice. If the coupling K_{xy} is set to zero, the coupling K_z constitutes a one-dimensional lattice. When the couplings are of equal strength, $K_{xy}=K_z$, the z direction, represented by the first embedding sequence, and the x,y directions, represented by

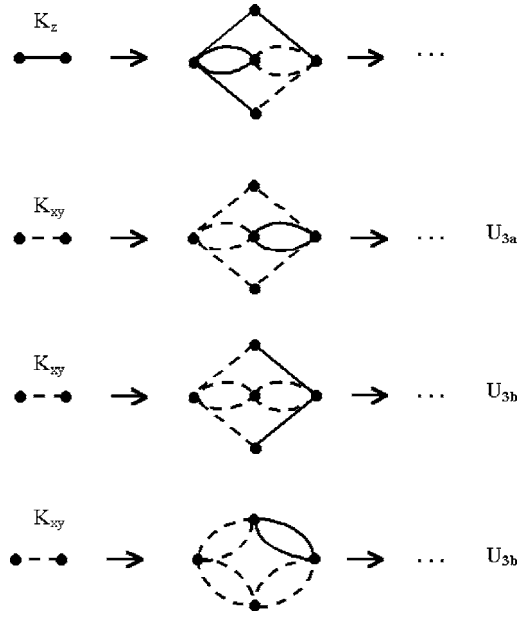

FIG. 3. The parallel, mutual embeddings of the top graph with either one of the following graphs provide uniaxially anisotropic $d=3$ hierarchical lattices. If the last graph is used, isotropy is not restored when $K_{xy}=K_z$. These lattices, differentiated by the choice of the second embedding graph, will be respectively referred to as U_{3a},U_{3b},U_{3c}.

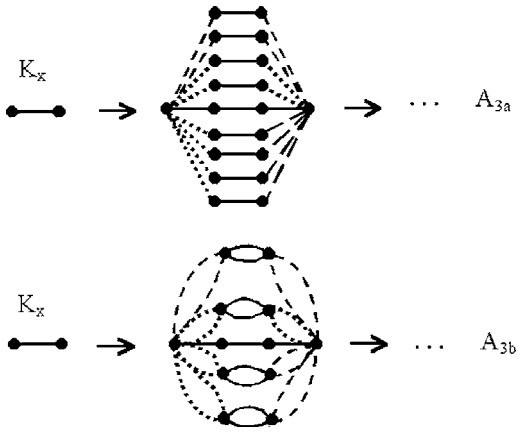

FIG. 4. Each embedding shown in this figure, in parallel with the two embeddings obtained by permuting K_x (full line), K_y (dashed), and K_z(dotted), yields a fully anisotropic $d=3$ hierarchical lattice. If any one the couplings K_u is set to zero, the remaining two couplings constitute an anisotropic two-dimensional lattice. If any two of the couplings are set to zero, the remaining coupling constitutes a one-dimensional lattice. When the couplings are of equal strength, $K_x=K_y=K_z$, the three directions, represented by the three mutual embedding sequences, are equivalent and the lattice is isotropic $d=3$. These lattices will be respectively referred to as A_{3a} and A_{3b}.

the second embedding sequence, are all equivalent and the lattice is isotropic $d=3$. This lattice will be referred to as U_3. In Fig. 3, the parallel, mutual embeddings of the top graph with either one of the following graphs also provide uniaxially anisotropic $d=3$ hierarchical lattices. If the last graph is used, isotropy is not restored when $K_{xy}=K_z$; this lattice is nevertheless included, for comparison, in our study. These lattices, differentiated by the choice of the second embedding graph, will be respectively referred to as U_{3a},U_{3b},U_{3c}.

A fully anisotropic $d=3$ hierarchical lattice is provided in Fig. 4 by each shown embedding in parallel with the two embeddings obtained by permuting K_x (full line), K_y (dashed), and K_z (dotted). If any one of the couplings K_u is set to zero, the remaining two couplings constitute an anisotropic two-dimensional lattice. If any two of the couplings are set to zero, the remaining coupling constitutes a one-dimensional lattice. When the couplings are of equal strength, $K_x=K_y=K_z$, the three directions, represented by the three embedding sequences, are equivalent and the lattice is isotropic $d=3$. These lattices will be referred to as A_{3a} and A_{3b}.

The anisotropic systems that we study are located on the anisotropic lattices constructed above. These hierarchical models admit exact renormalization-group solutions, with recursion relations obtained by decimations in direction opposite to their construction direction. The exact solutions of hierarchical models can simultaneously be considered approximate position-space renormalization-group solutions of models on naturally occurring lattices. In fact, the recursion relations obtained for the models below correspond to Migdal-Kadanoff [17,18] approximate recursion relations, which are hereby generalized to anisotropic systems.

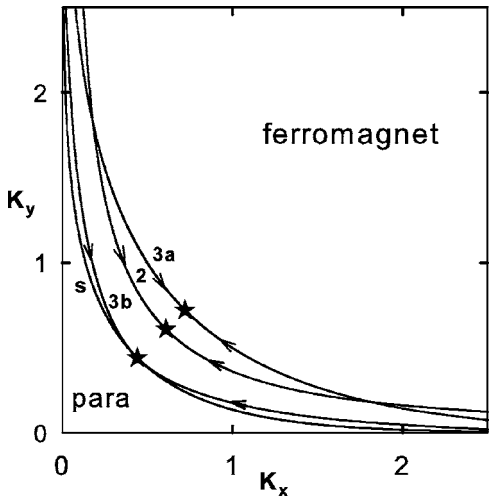

FIG. 5. The phase boundaries for the Ising model on the $d=2$ anisotropic hierarchical lattices A_2, A_{3a}, and A_{3b} (setting $K_z=0$) and the exact result [19] for the anisotropic square lattice (s). The arrows and stars, respectively, indicate the renormalization-group flows and fixed points.

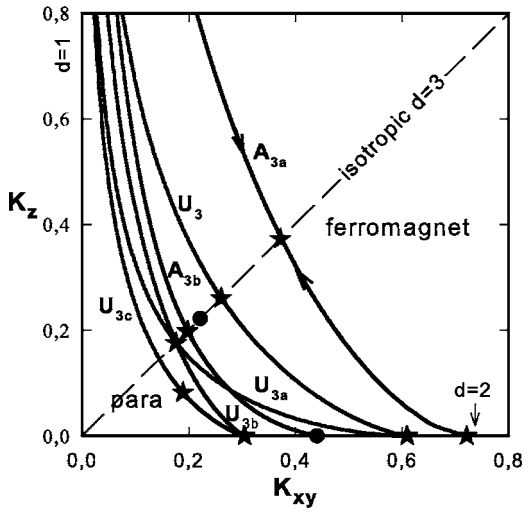

FIG. 6. Phase boundaries for the Ising model on the $d=3$ uniaxially anisotropic hierarchical lattices U_3, U_{3a}, U_{3b}, U_{3c}, A_{3a}, and A_{3b} (setting $K_x=K_y$). The exact phase transition points for the square [19] and cubic [20] lattices are shown by the black circles. For each model, the phase transitions at $d=1$ (at infinite coupling) and $d=2$ cross over (as shown for A_{3a}) to $d=3$ criticality, which is thus universal for all $d=3$ anisotropic and the $d=3$ isotropic cases. The $d=2$ fixed point of A_{3b} is not marked by a star, since it coincides with the square lattice exact transition point, marked by the black circle on the horizontal axis.

III. ANISOTROPIC ISING MAGNETS

The Ising model is defined by the Hamiltonian

$$-\beta H=\sum_u K_u \sum_{\langle ij\rangle_u} s_i s_j, \tag{1}$$

where, at each lattice site i, $s_i=\pm 1$, and $\langle ij\rangle_u$ denotes summation over bonds of type u. The various decimations in the models are composed of two elementary steps, $K=K_u+K_v$ for bonds in parallel and $K=\tanh^{-1}(\tanh K_u+\tanh K_v)$ for bonds in series, where K is the effective coupling of the combined bonds.

The phase boundaries for the Ising model on the $d=2$ anisotropic hierarchical lattices A_2, A_{3a}, and A_{3b} (setting $K_z=0$ in the latter two) are given in Fig. 5, along with the exact result for the anisotropic square lattice [19]. The renormalization-group flows are indicated on the phase boundary of the hierarchical models. The fixed point occurs at isotropy, $K_x=K_y$, to which the $d=2$ anisotropic critical points flow, thereby sharing the same critical exponents.

The phase boundaries for the Ising model on the $d=3$ uniaxially anisotropic hierarchical lattices U_3, U_{3a}, U_{3b}, U_{3c}, A_{3a}, and A_{3b} (setting $K_x=K_y$) are given in Fig. 6. The exact phase transition points for the square [19] and cubic [20] lattices are also shown. For each model, the phase transitions at $d=1$ (at infinite coupling) and $d=2$ cross over to $d=3$ criticality, which is thus universal for all $d=3$ anisotropic and the $d=3$ isotropic cases.

The phase boundary surface for the Ising model on the $d=3$ fully anisotropic hierarchical lattice A_{3b} is given in Fig. 7. The dashed lines on the planes are the exact $d=2$ solutions for the square lattice [19]. Again, all points on the critical surface of the $d=3$ fully anisotropic model flow onto the fixed point located at isotropy, thereby sharing its critical exponents. The critical exponents found for this model are $y_T=0.69$, $y_H=1.68$ for $d=2$ (for the square lattice $y_T=1$, $y_H=1.875$ [19]) and $y_T=0.92$, $y_H=2.20$ for $d=3$ (for the cubic lattice $y_T=1.59$, $y_H=2.50$ [21,22]).

IV. ANISOTROPIC *XY* MAGNETS

The XY model is defined by the Hamiltonian

$$-\beta H=\sum_u J_u \sum_{\langle ij\rangle_u} \mathbf{s}_i\cdot\mathbf{s}_j=\sum_u J_u \sum_{\langle ij\rangle_u}\cos(\theta_i-\theta_j), \tag{2}$$

where at each lattice site i, $\mathbf{s}_i$ is a unit vector confined to the xy plane at angle θ_i to the x axis and $\langle ij\rangle_u$ denotes summation

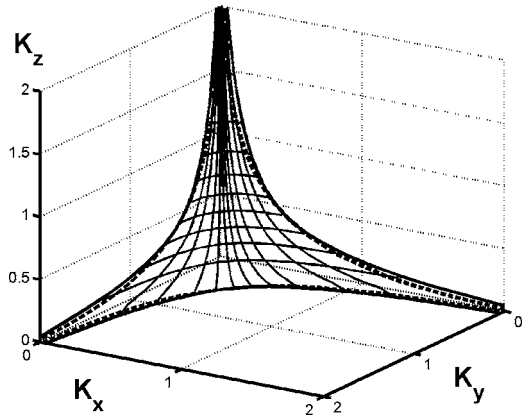

FIG. 7. Phase boundary surface for the Ising model on the $d=3$ fully anisotropic hierarchical lattice A_{3b}. The dashed lines on the planes are the exact $d=2$ solutions for the square lattice [19].

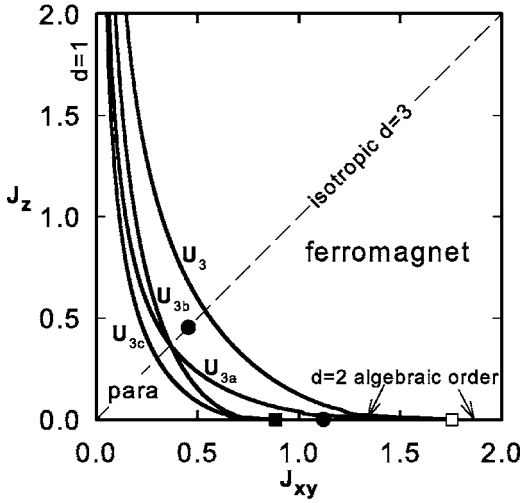

FIG. 8. Phase boundaries for the XY model on the $d=3$ uniaxially anisotropic hierarchical lattices U_3, U_{3a}, U_{3b}, and U_{3c}. The exact phase transition points for the square [23] and cubic [24] lattices are shown by the black circles. For each model, the phase transitions at $d=1$ (at infinite coupling) and $d=2$ (onset of algebraic order) cross over to $d=3$ criticality, which is thus universal for all $d=3$ anisotropic and the $d=3$ isotropic cases. The onsets of effective algebraic order in $d=2$ are marked, for models U_3, U_{3a} with the open square and for models U_{3b}, U_{3c} with the full square.

over bonds of type u. Under renormalization-group transformations, the coupling between nearest-neighbor sites takes the general form of a function $V_u(\theta_i-\theta_j)$. The various decimations in the models are composed of two elementary steps,

$$V = V_u + V_v,$$

$$V(\theta_i - \theta_k) = \ln \int_0^{2\pi} d\theta_j \exp[V_u(\theta_i - \theta_j) + V_v(\theta_j - \theta_k)], \quad (3)$$

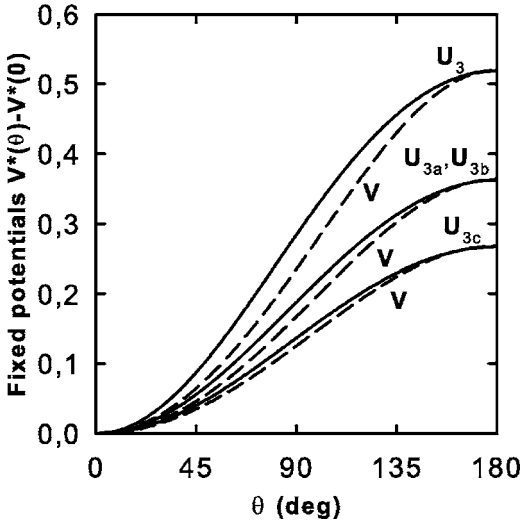

FIG. 9. Fixed potentials attracting the critical surface of the $d=3$ XY model. For comparison, appropriately normalized Villain potentials are also shown.

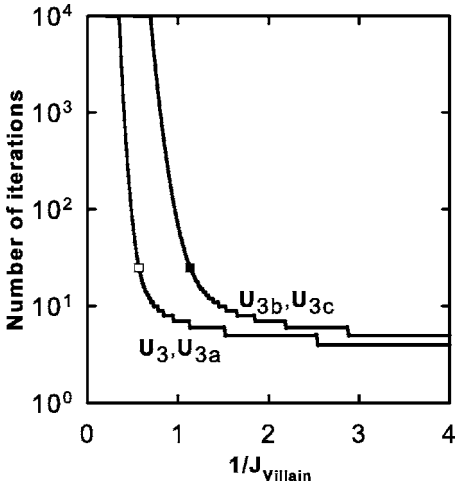

FIG. 10. Number of renormalization-group iterations necessary, in the $d=2$ XY model, for the Villain potential parametrized by J_V to decay to a disordered sink with $V(\theta)_{max}-V(\theta)_{min}<10^{-4}$. The squares indicate the onset of effective algebraic order.

respectively for bonds in parallel and in series, where V is the effective coupling of the combined bonds. In terms of Fourier components,

$$f_u(s) = \int_0^{2\pi} \frac{d\theta}{2\pi} e^{is\theta} \exp[V_u(\theta) - V_u(0)],$$

$$\exp[V_u(\theta) - V_u(0)] = \sum_s e^{-is\theta} f_u(s), \quad (4)$$

Eqs. (3) respectively are

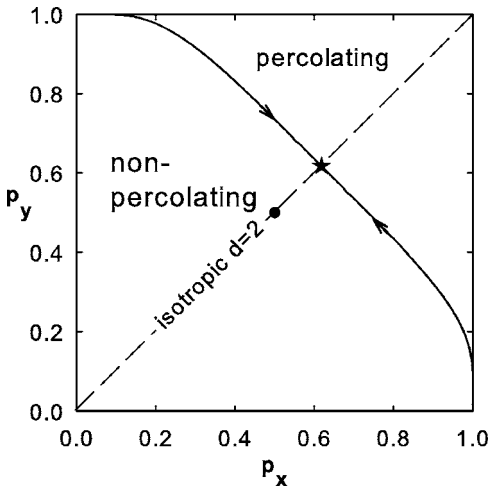

FIG. 11. The phase boundaries for percolation on the $d=2$ anisotropic hierarchical lattice (A_2). The renormalization-group flows are indicated on the phase boundary of the hierarchical model. The onset of percolation for the square lattice [29] is shown by the black circle.

$$f(s) = \sum_p f_u(p) f_v(s-p),$$

$$f(s) = f_u(s) f_v(s), \tag{5}$$

in a form that is more conveniently followed in our calculations. The phase boundaries for the XY model on the $d=3$ uniaxially anisotropic hierarchical lattices U_3, U_{3a}, U_{3b}, and U_{3c} are given in Fig. 8. The exact phase transition points for the square [23] and cubic [24] lattices are also shown.

In $d=2$, namely along the horizontal axis, above a critical interaction strength marked by the squares on the figure, the systems exhibit algebraic order [25–27]: The starting Hamiltonian [Eq. (2)] flows to a Villain potential [28],

$$f_V(s) = A \exp(-s^2/2J_V), \tag{6}$$

exhibiting a fixed-line behavior parametrized by J_V. This corresponds to a system without true long-range order, namely with zero magnetization, but infinite correlation length and algebraic order in which the correlations decay as a power law. In $d=3$, true long-range order occurs: points in the ferromagnetic phase renormalize to a δ function potential; points on the phase boundaries renormalize to single true fixed potential, shown in Fig. 9, differing from the Villain potential as also seen on the figure. The behavior here for $d=2$ is not true fixed-line behavior. After tens of thousands of renormalization-group iterations (corresponding to a scale change factor of 210 000), the Villain potential decays [27] to a disordered sink with $V(\theta)_{max} - V(\theta)_{min} < 10^{-4}$. The sharp change in the necessary number of iterations, as seen in Fig. 10, indicates the onset of effective algebraic order.

As seen in Fig. 8, for each XY model, the phase transitions at $d=1$ (at infinite coupling) and $d=2$ (onset of algebraic order) cross over to $d=3$ criticality, which is thus universal for all $d=3$ anisotropic and the $d=3$ isotropic cases.

V. ANISOTROPIC PERCOLATION

Anisotropic percolation is defined such that on each connection of direction u, a bond exist with probability p_u. The various decimations in the models are composed of two elementary steps, $p = p_u p_v + p_u(1-p_v) + p_v(1-p_u)$ for connections in parallel and $p = p_u p_v$ for connections in series, where p is the effective connectedness probability of the combined connections. The phase diagram for percolation on the $d=2$ anisotropic hierarchical lattice (A_2) is given in Fig. 11. The percolation fixed point occurs at isotropy, $p_x = p_y$, to which the $d=2$ anisotropic percolation onsets flow, thereby sharing the same critical exponents. The phase boundaries for percolation on the $d=3$ uniaxially anisotropic hierarchical lattices U_3, U_{3a}, U_{3b}, and U_{3c} are given in Fig. 12. The percolation points for the cubic and square lattices are also shown [29]. For each model, percolation onset at $d=1$ (at $p_z=1$) and $d=2$ cross over to $d=3$ percolation onset, which is thus universal for all $d=3$ anisotropic and the $d=3$ isotropic cases.

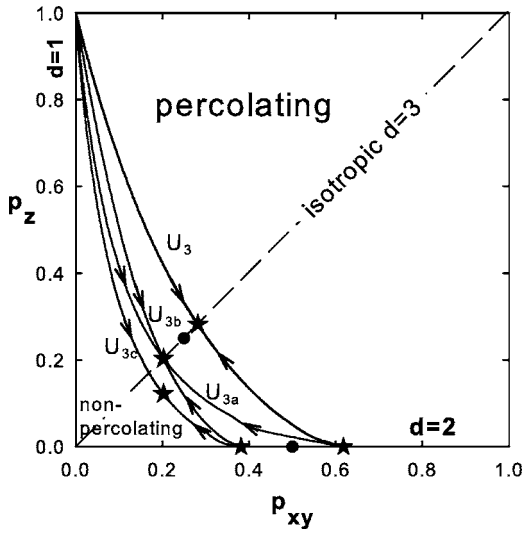

FIG. 12. Phase boundaries for percolation on the $d=3$ uniaxially anisotropic hierarchical lattices U_3, U_{3a}, U_{3b}, and U_{3c}. The onsets of percolation for the square and cubic lattices [29] are shown by the black circles. For each model, the percolation onset at $d=1$ (at $p_z=1$) and $d=2$ cross over to $d=3$ percolation onset, which is thus universal for all $d=3$ anisotropic and the $d=3$ isotropic cases.

ACKNOWLEDGMENTS

This research was supported by the Scientific and Technical Research Council of Turkey (TÜBITAK) and by the Academy of Sciences of Turkey.

[1] A. N. Berker and S. Ostlund, J. Phys. C **12**, 4961 (1979).
[2] M. Kaufman and R. B. Griffiths, Phys. Rev. B **24**, R496 (1981).
[3] M. Kaufman and R. B. Griffiths, Phys. Rev. B **30**, 244 (1984).
[4] A. Falicov and A. N. Berker, Phys. Rev. B **51**, 12458 (1995).
[5] M. Hinczewski and A. N. Berker, e-print cond-mat/0503226.
[6] M. Hinczewski and A. N. Berker, e-print cond-mat/0503631.
[7] S. R. McKay, A. N. Berker, and S. Kirkpatrick, Phys. Rev. Lett. **48**, 767 (1982).
[8] G. Migliorini and A. N. Berker, Phys. Rev. B **57**, 426 (1998).
[9] D. Andelman and A. N. Berker, Phys. Rev. B **29**, 2630 (1984).
[10] A. Falicov, A. N. Berker, and S. R. McKay, Phys. Rev. B **51**, 8266 (1995).
[11] E. Domany, S. Alexander, D. Bensimon, and L. P. Kadanoff, Phys. Rev. B **28**, 3110 (1983).
[12] J.-M. Langlois, A.-M. S. Tremblay, and B. W. Southern, Phys. Rev. B **28**, 218 (1983).
[13] R. B. Stinchcombe and A. C. Maggs, J. Phys. A **19**, 1949 (1986).
[14] T. A. S. Haddad, S. T. R. Pinho, and S. R. Salinas, Phys. Rev. E **61**, 3330 (2000).
[15] J.-X. Le and Z. R. Yang, Phys. Rev. E **69**, 066107 (2004).
[16] R. A. da Silveira and J.-P. Bouchaud, Phys. Rev. Lett. **93**, 015901 (2004).

[17] A. A. Migdal, Zh. Eksp. Teor. Fiz. **69**, 1457 (1975) [Sov. Phys. JETP **42**, 743 (1976)].
[18] L. P. Kadanoff, Ann. Phys. (N.Y.) **100**, 359 (1976).
[19] L. Onsager, Phys. Rev. **65**, 117 (1944).
[20] A. M. Ferrenberg and D. P. Landau, Phys. Rev. B **44**, 5081 (1991).
[21] M. A. Moore, D. Jasnow, and M. Wortis, Phys. Rev. Lett. **22**, 940 (1969).
[22] D. S. Gaunt and M. F. Sykes, J. Phys. C **5**, 1429 (1972).
[23] M. Hasenbusch, J. Phys. A **38**, 5869 (2005).
[24] M. Ferer, M. A. Moore, and M. Wortis, Phys. Rev. B **8**, 5205 (1973).
[25] J. M. Kosterlitz and D. J. Thouless, J. Phys. C **6**, 1181 (1973).
[26] J. V. José, L. P. Kadanoff, S. Kirkpatrick, and D. R. Nelson, Phys. Rev. B **16**, 1217 (1977).
[27] A. N. Berker and D. R. Nelson, Phys. Rev. B **19**, 2488 (1979).
[28] J. Villain, J. Phys. (Paris) **36**, 581 (1975).
[29] J. W. Essam, in *Phase Transitions and Critical Phenomena*, edited by C. Domb and M. S. Green (Academic, London, 1972), Vol.2, pp. 197–270.